Journal of Solid State Chemistry 184 (2011) 1707–1714

Contents lists available at ScienceDirect

Journal of Solid State Chemistry

journal homepage: www.elsevier.com/locate/jssc

Luminescence of Tb-doped $Ca_3Y_2(Si_3O_9)_2$ oxide upon UV and VUV synchrotron radiation excitation

Anna Dobrowolska, Eugeniusz Zych*

Faculty of Chemistry, University of Wroclaw, 14. F. Joliot-Curie Street, 50-383 Wroclaw, Poland

ARTICLE INFO

Article history:
Received 28 February 2011
Received in revised form
5 May 2011
Accepted 7 May 2011
Available online 14 May 2011

Keywords:
Calcium yttrium silicate
Tb^{3+} luminescence
VUV excitation
Exciton

ABSTRACT

Powders of calcium yttrium silicate, $Ca_3Y_2(Si_3O_9)_2$, containing 0.1–3% Tb^{3+} were prepared using a sol-gel method and characterized with XRD, IR, UV–vis and UV–VUV spectroscopies at room temperature and 10 K. Structural analysis revealed pure monoclinic phase of $Ca_3Y_2(Si_3O_9)_2$ after heat-treatment at 1000 °C. Infrared spectroscopy showed that between 800 and 900 °C a short-range structural organization of the components proceeded, yet without crystallization. A strong emission of Tb^{3+} had been observed both in the green part of the spectrum due to the $^5D_4 \rightarrow {}^7F_J$ transitions and in the blue-violet region owing to the $^5D_3 \rightarrow {}^7F_J$ radiative relaxation. The color of the light could be tuned from yellowish-green to bluish-white both by means of the dopant content and the temperature of synthesis. Efficient luminescence of Tb^{3+}-doped $Ca_3Y_2(Si_3O_9)_2$ phosphors could also be obtained upon stimulation with vacuum ultraviolet synchrotron radiation demonstrating that an energy transfer from the host to the Tb^{3+} ions takes place.

1. Introduction

Yamane et al. [1] reported on a layered structure of a monoclinic $Ca_3Y_2(Si_3O_9)_2$ with $C2/c$ space group. Ca and Y atoms randomly share 6-, 7- and 8-fold coordination symmetry sites in this composition (Fig. 1). Consequently, dopants introduced into the host also reside in the different positions. The structure of $Ca_3Y_2(Si_3O_9)_2$ can be seen as an arrangement of two types of layers, one of which assembles metal ions (Ca^{2+}/Y^{3+}), while the other consists of SiO_4 tetrahedrons. Both layers are stacked along the [10−1] direction. Two oxygen atoms of every SiO_4 tetrahedron are shared with another SiO_4 tetrahedron resulting in the formation of ternary Si_3O_9 rings with Ca/Y atoms coupled with them (Fig. 1, [2]). Such an arrangement of the metal ions reduces their capability to interact, which in turn should open an opportunity to introduce a relatively high content of luminescent impurities without quenching of their emission [3].

Terbium-activated phosphors are usually excellent emitters of green light due to an effective excitation through the $4f \rightarrow 5d$ transitions covering a broad range of wavelengths and efficient $^5D_4 \rightarrow {}^7F_J$ luminescent transitions. The $^5D_4$ state is not prone to quenching and the $^5D_4 \rightarrow {}^7F_5$ emission around 545 nm is the strongest [4,5]. A substantial contribution from the more energetic $^5D_3 \rightarrow {}^7F_J$ luminescence in blue and near UV can also be occasionally observed. It is however susceptible to concentration quenching through cross-relaxation [4,13].

Two papers have been published on the issue of energy transfer between Ce^{3+} and Tb^{3+} in $Ca_3Y_2(Si_3O_9)_2$:Tb,Ce phosphor until now [6,7]. The present paper lays down the results of a spectroscopic investigation of a singly activated $Ca_3Y_2(Si_3O_9)_2$:Tb composition in VUV–UV–vis range of wavelengths at room temperature (RT) and 10 K. An in depth understanding of the spectroscopic properties of this singly activated composition will prove useful in the development of new $Ca_3Y_2(Si_3O_9)_2$-based phosphors deliberately.

2. Materials and methods

$Ca_3Y_2(Si_3O_9)_2$ powders doped with Tb^{3+} ions were prepared using sol–gel method described by Andric et al. [8] for $CaSiO_3$. CaO (99.6–100.5%, Riedel de Haen), Y_2O_3, (99.99%, Stanford Materials), Tb_4O_7 (99.999%, Stanford Materials) and TEOS (99.999%, Aldrich) were used as starting materials. Powders of the oxide substrates were pre-calcinated at 1000 °C in air atmosphere for 4 h in order to remove CO_2 and H_2O absorbed on their surface. The oxides were dissolved in nitric acid (65%) and ammonia was added to change the pH to 2. The mixture was thereafter combined with an ethanol solution of TEOS. As a result of a few hours of stirring at room temperature a sol was obtained and transferred into a dried gel within 5–10 h at 80 °C. Dried gels were heated in air at 800, 900 and 1000 °C for 4 h. After the first heat-treatment each powder was divided into two parts and one

* Corresponding author. Fax: +48 71 328 2348.
E-mail address: zych@wchuwr.pl (E. Zych).

0022-4596/$ - see front matter © 2011 Elsevier Inc. All rights reserved.
doi:10.1016/j.jssc.2011.05.014

of each portion was additionally calcinated in a reducing atmosphere of N_2 (75%)–H_2 (25%) mixture in Pt90%/Rh10% crucibles for 4 h accordingly.

Room temperature luminescence and luminescence excitation spectra were recorded with 0.2 nm resolution using FSL 920 Spectrometer from Edinburgh Instruments. The excitation spectra were taken with the emission monochromator slits set to 3 nm. 450 W Xe-lamp was used as an excitation source and both types of spectra were corrected for the system characteristics. Luminescence decay traces were recorded with the same instrument using its dedicated Xe flash lamp (60 W) as the excitation source. In the fitting procedure the deconvolution of the excitation pulse shape was applied using the instrument dedicated software. The X-ray diffraction (XRD) patterns were measured with D8 Advance diffractometer from Bruker using Cu$K\alpha$1 radiation (λ=1.540596 Å) in the range of 2θ=5–100° with $\Delta\theta$=0.016° step and counting time 8 s. FT-IR spectra were recorded with an IFS 66/s Bruker spectrometer in the range of 400–4000 cm^{-1}. The powders were diluted in KBr and nujol. The luminescence and luminescence excitation spectra were also recorded with synchrotron radiation at RT and 10 K at the Superlumi station of DESY-Hasylab in Hamburg (Germany). These luminescence spectra were recorded using a CCD camera with a resolution of about 0.25 nm. The synchrotron excitation spectra were corrected for the incident light intensity using sodium salicylate as a standard and the emissions were corrected for the spectral characteristics of the detection system.

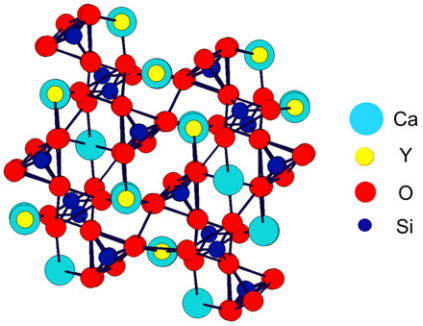

Fig. 1. Unit cell of $Ca_3Y_2(Si_3O_9)_2$ [3]. Ca and Y randomly occupy the same three sites of 6-, 7 and 8-fold coordination symmetries.

3. Results and discussion

Powders prepared in a N_2–H_2 mixture were snow-white, while those made in air exhibited a slight creamy hue. XRD patterns and IR spectra of all compositions were very similar. However, emission intensities, independent of the Tb content, were at least a few times lower for materials prepared in air. Therefore, only results for the reduced materials shall be presented.

3.1. Structural analysis

To investigate how the crystallization of the sol–gel derived powders of $Ca_3Y_2(Si_3O_9)_2$:Tb proceeds XRD technique and IR spectroscopy were employed. Structural measurements reveal that samples synthesized at 800 °C are amorphous, yet (Fig. 2a) their XRD patterns are dominated by two very broad bands located at around 30° and 45°. Increasing the preparation temperature to 900 °C initiates the crystallization (Fig. 2a). The broad structures still dominate the XRD pattern, yet diffraction lines characteristic for $Ca_3Y_2(Si_3O_9)_2$ oxide become already recordable. Intensities of the XRD lines of the powder are weak, indicating that only a small fraction of the material gets crystallized at 900 °C. Finally, after heat-treatment at 1000 °C a pure monoclinic phase with $C2/c$ space group appears (PDF-2 #01-087-0459) (Fig. 2a). A comparison of the XRD spectra for different concentrations of activator ions (not presented) proves that an addition of Tb up to 3% does not influence the crystallization process. Thermogravimetric analysis, not presented here, proves that above 700 °C no mass loss is observed (TG). Yet, on DTA curve an exothermic peak is observed at 1050 °C, which corresponds with the results of XRDs.

FT-IR spectra in the range of host-related vibrations (400–1400 cm^{-1}) for powders prepared at different temperatures (800–1000 °C) are presented in Fig. 2b. In the not presented range of 1400–4000 cm^{-1} no bands were observed, indicating that already at 800 °C neither water, OH^- nor organic residuals were left in the powders. This is crucial for the analysis of the luminescent results. The IR spectra reveal that the various vibrations systematically appear or become stronger and well defined as the temperature of preparation increases. The spectrum of the material made at 800 °C contains two broad structures peaking with absorption maxima around 500 and 950 cm^{-1}. Only after

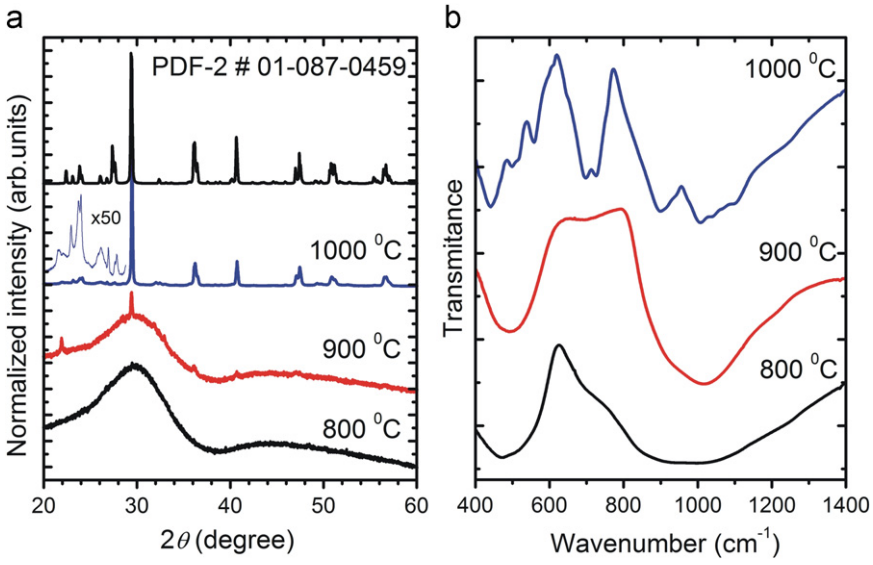

Fig. 2. XRD patterns for $Ca_3Y_2(Si_3O_9)_2$:Tb^{3+} powders after different heat-treatments (a) and their IR spectra (b).

the heat-treatment at 1000 °C, when the crystallization is complete, as concluded from XRDs, the IR spectrum consists of more numerous and much narrower components, which proves that only then all the chemical bonds and atomic interactions within the host are finally fully formed. According to [8,9] the components at 440, 510 and 560 cm^{-1} can be attributed to O–Si–O bond bending and metal–oxygen bond stretching mode vibrations and those at 695 and 720 cm^{-1} (absent in powders prepared below 1000 °C) to Si–O–Si bond bending and Si–O stretching vibrations, which can be taken as a sign of a silicate network formation. Absorption between 850 and 1200 cm^{-1} results from asymmetric Si–O stretching modes within SiO_4 tetrahedra. These data coincide with numbers received from Raman spectra (not presented here) that gave vibrations located at 418, 598, 987, 1041 and 1090 cm^{-1}, as well as very weak 2–3 components at around 650–720 cm^{-1}. These results support the conclusions drawn from XRDs and also point with higher precision to the difference in the structural organization of the atoms in materials made at 800 and 900 °C. The structural changes should exert their influence on the luminescent behavior of the materials as this property is, among others, a function of the local symmetry of the luminescent center.

3.2. Room temperature luminescence under UV excitation

Fig. 3 presents luminescence spectra of the Tb^{3+}-doped $Ca_3Y_2(Si_3O_9)_2$ phosphors under UV excitation as a function of the temperature of synthesis and concentration of activators ions. With the increase in temperature of the preparation the emission structures become narrower. This is especially evident comparing materials prepared at 900 and 1000 °C. This effect mirrors the enhancement of the structural ordering and increasing crystallinity, already proved by XRD and IR measurements. Yet, even for the material made at 1000 °C the luminescent features seems to be somewhat broader, and more numerous than typically observed in crystals. This may easily reflect the random distribution of the dopant within the three sites of different symmetries in the host lattice [6].

Stimulation into $4f^7 \rightarrow 4f^6 5d^1$ band (236 nm) of Tb^{3+} ions results at first in efficient nonradiative relaxation to the $^5D_3$ and possibly $^5D_4$ levels and subsequent UV-blue emission from the former (382–455 nm) and green luminescence from the latter (455–650 nm) [6,10,11]. The intensity ratio between emissions from $^5D_3$ and $^5D_4$ varies significantly with concentration of the Tb^{3+} ions in the lattice as well as with preparation temperature. Yet, for most powders the higher-energy emission from the $^5D_3$ state contains a significant, even prevalent part of the total luminescence intensity. Within the same concentration the comparative luminescence intensity from the $^5D_3$ state increases significantly with increase in temperature of preparation, hence with improvement in the organization of the structure.

Only in emission spectra for powders heat-treated at 800 °C the luminescence from the $^5D_4$ energy level prevails over that from the $^5D_3$, independently on the Tb^{3+} content. Yet, increasing the temperature of preparation to 900 °C leads to a significant relative amplification of the more energetic luminescent components connected with the $^5D_3$ level. This becomes more profound for materials prepared at 1000 °C. Hence, for powders prepared at 900–1000 °C the emission from the $^5D_3$ level comprises at least half of the total luminescence intensity even when the Tb content reaches 1%. For the 3% concentration of Tb the green luminescence appears stronger, yet even then the emission from $^5D_3$ constitutes about 30% of the total. Clearly, the energy from the $^5D_3$ level meets difficulties in lowering nonradiatively down to the $^5D_4$ level.

For the powders prepared at 800 °C the $^5D_3$ state contributes in a noticeably lower degree to the total luminescence. This can be attributed to the fact that at such low temperature of preparation the materials gain neither crystallinity, as was seen in XRDs, nor any short-distance arrangements of the constituting atoms, as was observed by IR spectroscopy. Consequently, the Tb dopant may easily form clusters and/or may preferentially situate mostly on the grain surfaces and thus be exposed to interactions enhancing various nonradiative pathways [12]. In these materials enhanced population of defects can also be expected, which may open additional channels for nonradiative processes and thus quench the luminescence [13]. Indeed, the total efficiency of emission of materials prepared at 800 °C is more than an order of magnitude lower than from the analogous compositions synthesized at 900–1000 °C (though detailed measurements of efficiencies have not yet been performed). Hence, altogether the picture is consistent. When the preparation temperature increases

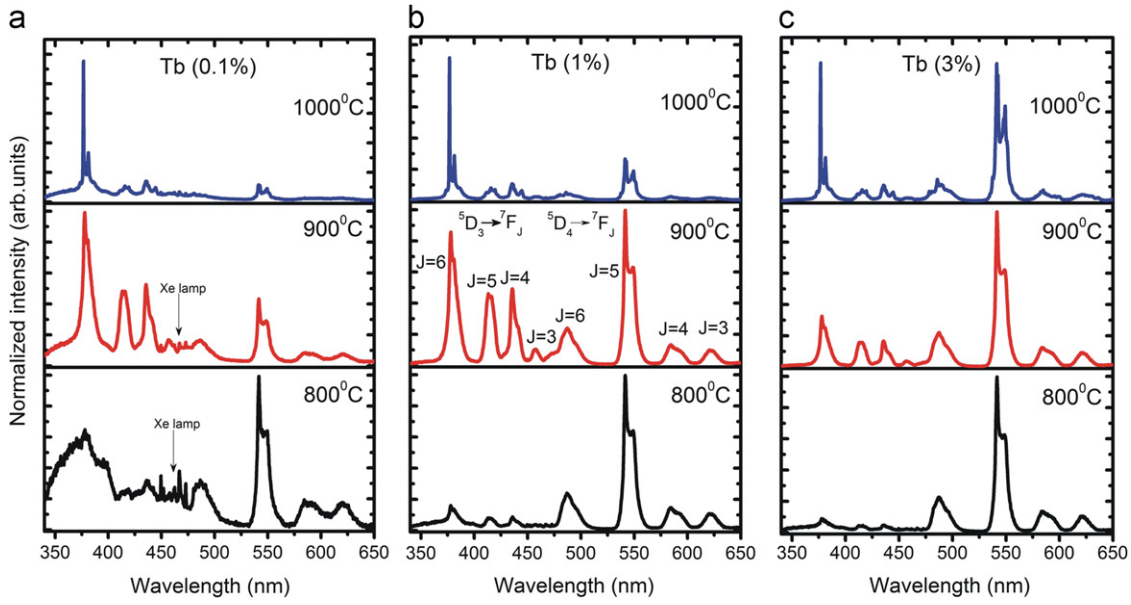

Fig. 3. Luminescence spectra of $Ca_3Y_2(Si_3O_9)_2$:Tb powders synthesized at 800, 900 and 1000 °C containing 0.1% (a), 1% (b) and 3% (c) of Tb. Spectra were taken under 236 nm radiation. Transition assignments are given in the central segment. Some scattered excitation light is seen in the spectra of 0.1% specimens made at 800 and 900 °C.

leading to a development of the network of bonds within the host material and finally to its crystallization, the Tb activator may get uniformly dissolved within it and thus the overall efficiency of luminescence boosts and the $^5D_3$ emission becomes dominant. At high Tb contents (3%) the cross-relaxation can additionally drain the energy from $^5D_3$ to $^5D_4$ level enhancing efficiency of the green luminescence at the expense of the blue-near UV one [14]. It is striking that the quenching of $^5D_3$ emission becomes evident at a rather high content of Tb^{3+} (3%) (this will be visible in the kinetics measurements). It is, however, reasonable taking into account the structure of the host material. The three metal ions symmetry sites are quite well isolated from each other by various SiO_4 tetrahedrons as it was discussed in Section 1. In such circumstances the interaction between ions of the dopant is hindered and the nonradiative feeding of the $^5D_4$ state through cross-relaxation gets hampered.

Typical excitation spectrum of 541.4 nm ($^5D_4 \rightarrow {}^7F_5$) luminescence of $Ca_3Y_2(Si_3O_9)_2$:Tb^{3+} phosphors (Fig. 4) is composed of broad components located in the range of 220–300 nm attributed to $4f \rightarrow 5d$ transitions of the dopant and a whole set of lines ascribed to absorption within its $4f^8$ shell. The $4f \rightarrow 5d$ excitation features can be clearly divided into spin allowed with the peak positioned at around 233 nm (42 900 cm^{-1}), and spin forbidden located at around 268 (37 700 cm^{-1}) and 253 nm. The energies of the lowest $4f \rightarrow 5d$ transitions, spin allowed and spin forbidden, agree perfectly with the predictions given by Dorenbos [15]. The energy of the lowest $4f \rightarrow 5d$ (320 nm, 31 250 cm^{-1}) was taken from [6]. This again confirms the usability of the Dorenbos' method. The appearance of the spin-allowed and spin-forbidden transitions is a result of an exchange interaction between seven aligned spins of $4f$ electrons and the spin of the excited $5d$ electron [3,16,17]. At wavelengths longer than about 300 nm the $4f \rightarrow 4f$ transitions produce low-intensity narrow excitation structures. Their assignment is given in Fig. 4 [6,11,14,18].

3.3. Decay kinetics

Since from luminescent spectra a concentration dependence of the $^5D_3 \rightarrow {}^5D_4$ nonradiative energy transfer was revealed, measurements of decay kinetics of emissions from both these states were performed, where needed average time constants were

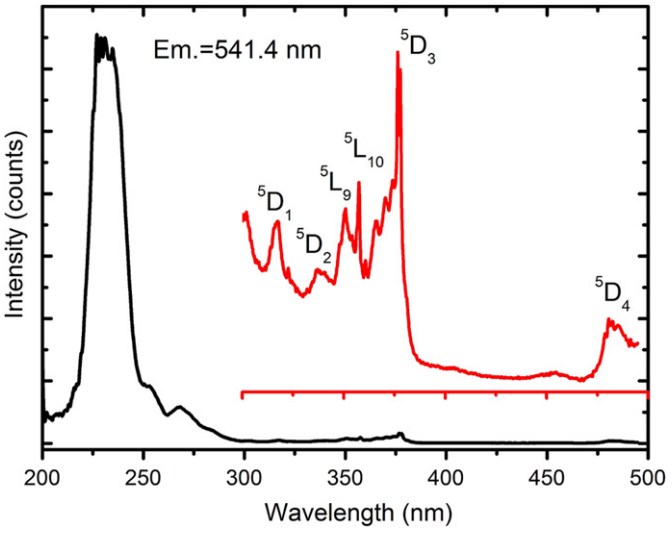

Fig. 4. Excitation spectrum of $^5D_4 \rightarrow {}^7F_5$ luminescence of Tb^{3+} monitored at 541.4 nm. Inset in the graph shows the $4f \rightarrow 4f$ transitions of Tb^{3+} ions and gives the terminal levels of the absorption from the $^7F_6$ ground state.

Table 1
Basic kinetic parameters derived from fitting the luminescence decay traces of 377 and 543 nm emissions in $Ca_3Y_2(Si_3O_9)_2$:Tb(x %) samples prepared at different temperatures.

Tb^{3+} (mol%)	Synthesis temperature (°C)	Emission		
		Em. = 543 nm		Em. = 377 nm
		Rise time (ms)	$\langle\tau\rangle$ (ms)	$\langle\tau\rangle$ (ms)
0.1	**800**	0.4	3.9	0.5
	900	0.6	2.8	1.2
	1000	1.5	8.1	4.2
1	**800**	2.5	3.9	0.6
	900	4.3	2.8	1.0
	1000	4.0	7.4	3.6
3	**800**	2.0	3.8	0.4
	900	2.7	2.5	0.6
	1000	3.6	6.5	2.4

calculated (Table 1) according to [19,20]:

$$\langle\tau\rangle = \frac{\int_0^\infty tI(t)\mathrm{d}t}{\int_0^\infty I(t)\mathrm{d}t} \quad (1)$$

Systematic changes occur in the decay traces (Fig. 5). Within the same concentration the $^5D_3$ emissions become progressively longer with increase in preparation temperature, which accords with and substantiates the conclusions drawn from XRDs and IR spectra on a continuous growing of structural organization of the materials with an increase in synthesis temperature. For the lowest Tb content (0.1%) decay of the $^5D_3$ luminescence (377 nm) becomes progressively more exponential with increase in temperature of preparation to turn into a single exponential at 1000 °C. For higher concentrations of the activator the decays of the $^5D_3$ luminescence shorten indicating increase in draining the energy from $^5D_3$ to $^5D_4$. This behavior perfectly mirrors continuous lessening of the $^5D_3$ luminescence relative intensity compared to the $^5D_4$ one, as is seen in Fig. 3.

The decay traces of the Tb^{3+} green emissions from $^5D_4$ state are close to a single exponential form for all materials. In all those traces a significant rise of the signal is observed. This confirms that energy from $^5D_3$ goes to $^5D_4$ (mainly) through a relatively slow nonradiative process, presumably cross-relaxation. It should be noted that the green luminescence from $^5D_4$ appears the fastest for specimens made at 900 °C, while for the $^5D_3$ emission the fastest luminescence was for materials made at 800 °C. Additionally, kinetics of the green emission is hardly dependent on Tb content, no matter what the preparation temperature was. It is intriguing that the powder made at 900 °C produces definitely the strongest luminescence amongst the investigated materials. Hence, its relatively short decay time does not seem to reflect quenching processes but echoes an increased probability of the $^5D_4 \rightarrow {}^7F_5$ radiative relaxation rather. This effect has to be somehow connected with the just formed at 900 °C, a short-range organization of the structure, but in principle without crystallization yet.

3.4. Room temperature and 10 K luminescence under VUV–UV synchrotron radiation excitation

Luminescence and luminescence excitation spectra for powders containing 1% of Tb^{3+} synthesized at 900 and 1000 °C were recorded at room temperature (RT) and 10 K. The excitation spectra of various luminescent features are presented in Fig. 6.

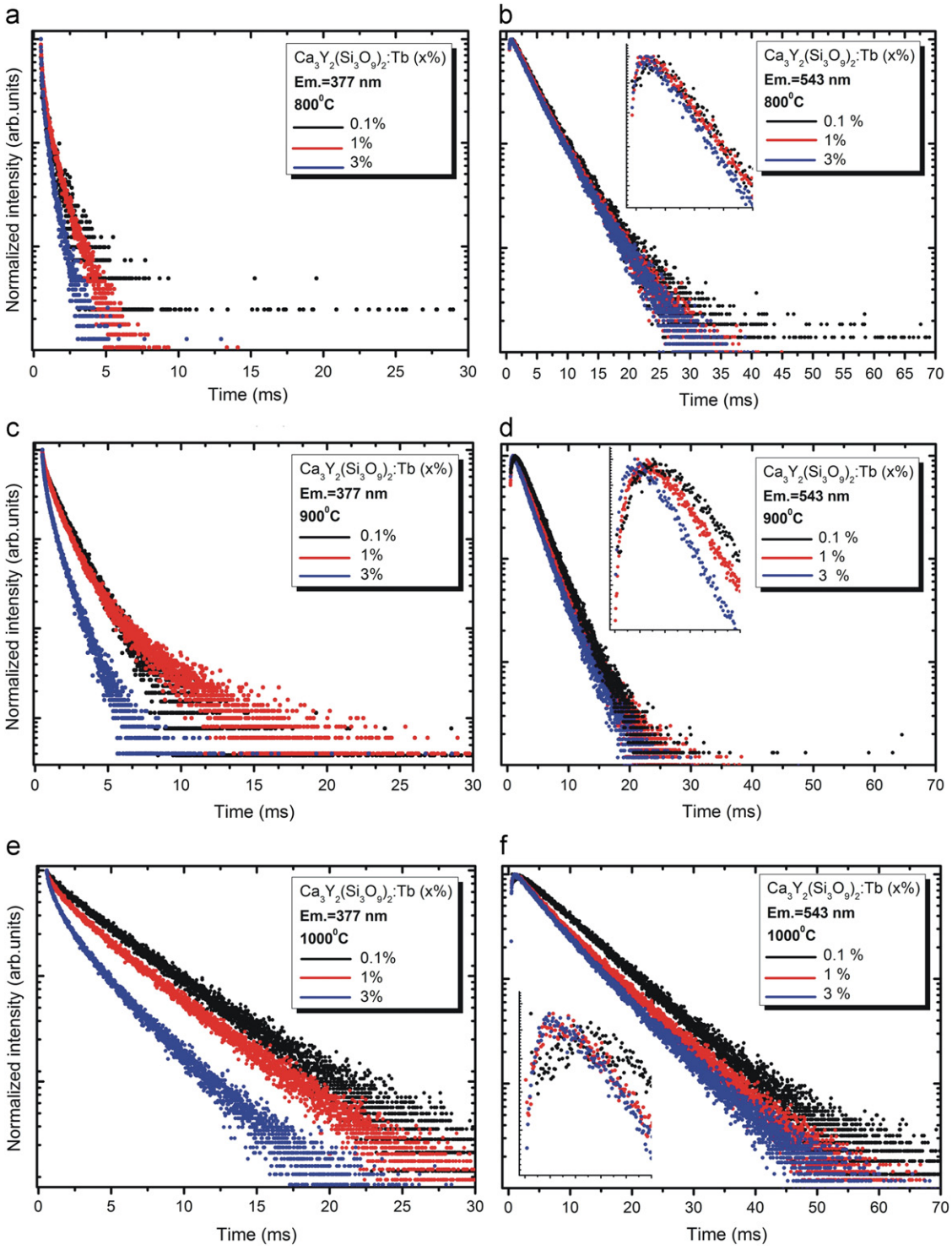

Fig. 5. Luminescence decay traces of emission from $^5D_3$ (a, c, e) and $^5D_4$ (b, d, f) levels upon excitation with 236 nm wavelength radiation. In the insets the first 2.5 ms of the traces is shown to better expose the rise of the signals.

Excitation spectra of emissions form $^5D_3$ (382 nm) and $^5D_4$ (542 nm) taken at 10 K (Fig. 6b and d) consist of two broad bands located at around 230 and 175 nm for both types of powders. Since the spectra have analogous characteristics only the latter will be further presented. The higher-energy band is the only strong component appearing in the excitation spectrum of the 365 nm broad-band luminescence at 10 K, which is presented in Fig. 7d. The lower energy band (230 nm) was already (Fig. 4) assigned to the allowed $4f^8 \rightarrow 4f^7 5d^1$ absorption of Tb^{3+}. The band peaking at 175 nm is assumed to result from the fundamental absorption of the host material. Yet, according to [16,21], it may envelope the $O^{2-} \rightarrow Tb^{3+}$ charge transfer absorption band. At room temperature (Fig. 6a and c) excitation spectra of both Tb emissions (377 and 542 nm) of the (almost noncrystalline) powder prepared at 900 °C are dominated by the band around 230 nm and the band around 175 nm exists only in a residual form. The situation changes noticeably when the preparation is performed at 1000 °C and the powder is crystallized. RT excitation

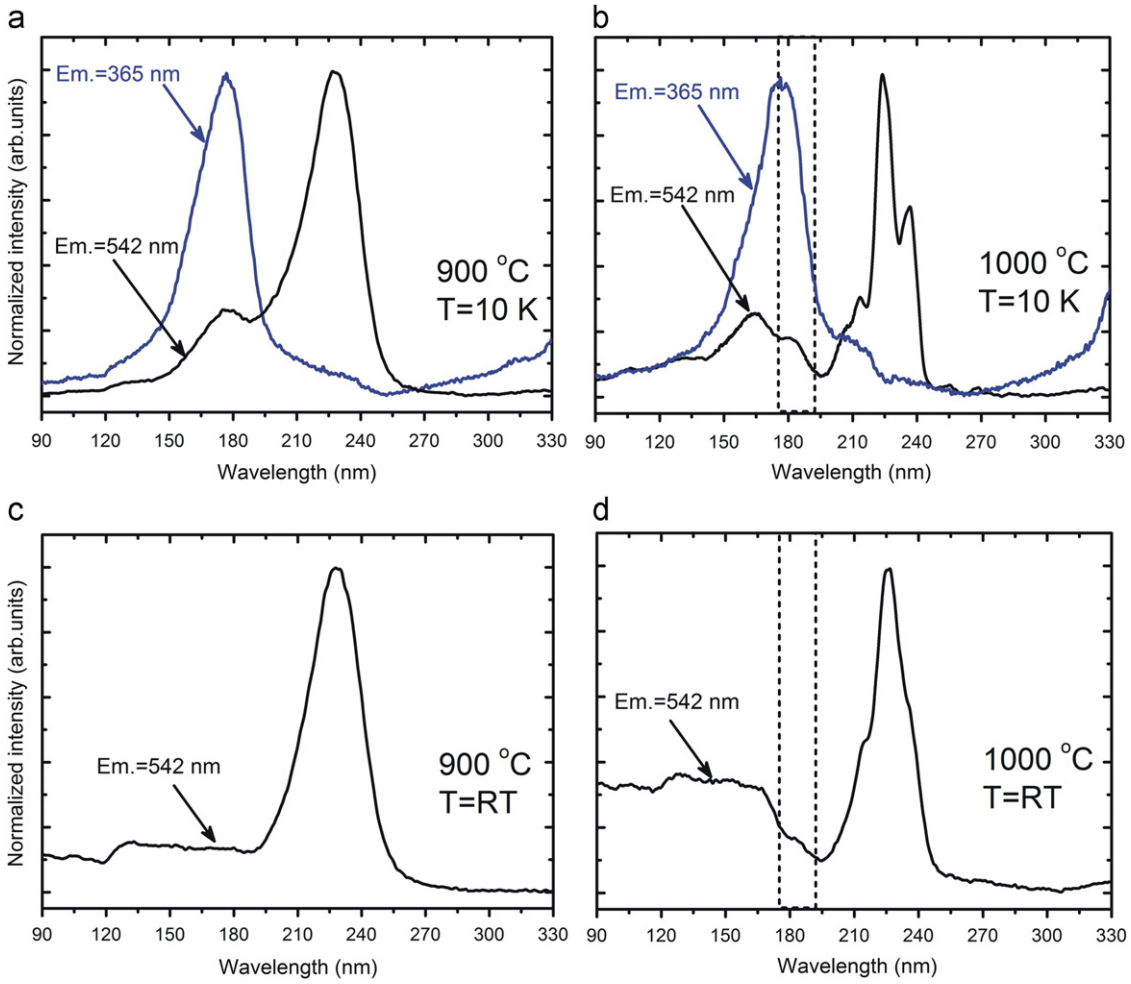

Fig. 6. RT and 10 K excitation spectra of the main luminescent features positioned at 365 nm (only 10 K) and 542 nm in the $Ca_3Y_2(Si_3O_9)_2$:Tb (1%) powders prepared at 900 °C (a, c) and 1000 °C (b, d).

spectrum of Tb luminescence contains a broad band of a significant intensity extending from about 175 nm well into deep VUV region. Its relative intensity compared to the $4f \rightarrow 5d$ feature at around 230 nm is at least an order of magnitude higher than for a material made at 900 °C. The presence of this intense band in excitation spectra of Tb^{3+} luminescence indicates that energy from the excited host is being efficiently transferred to the dopant. The basically amorphous lattice in the material synthesized at 900 °C is able to support such a transfer of energy with a lesser efficacy. There is yet another difference in the excitation spectra of the almost amorphous (900 °C) and crystalline (1000 °C) powders. In the crystalline material the excitation features are clearly structured, especially those related to the $4f \rightarrow 5d$ transitions, while in the almost amorphous phosphor they are all inhomogeneously broadened to such an extent that smooth broad bands without any distinguished components are formed even at 10 K.

A more detailed inspection of the excitation spectra of the crystalline (1000 °C) powder at RT and 10 K allows for additional conclusions. Typically, the position of the onset of the band-to-band excitation shifts towards higher energies (shorter wavelengths) when the temperature decreases. In the spectra presented in Fig. 6b and d an opposite effect occurs (see the areas marked with broken lines). In the region of the bang-gap the room temperature excitation spectrum (almost) lacks a component located in the range of about 175–190 nm. This location coincides with the low-energy part of the excitation band of the 365 nm broad luminescence seen only at 10 K. Altogether, it seems that the 175–190 nm component appears as a significant feature only in the 10 K excitation spectra of both the Tb^{3+} emission and the broad band luminescence peaking at around 365 nm. At RT this excitation produces neither the broad nor the Tb^{3+} luminescence. These observations can be rationalized in such a way that the 175–190 nm feature is connected with an excitonic state stable only at a low temperature. Therefore at 10 K it appears in the excitation spectra of both the Tb^{3+} luminescence and the broad-band emission peaking at around 365 nm. The relative intensity of the 365 nm luminescence is higher for materials made at 900 °C compared to the crystalline powder prepared at 1000 °C. This may reflect a higher population of lattice defects in the former sample serving as relaxation centers for excitons.

The above findings and differences between the two materials made at 900 and 1000 °C are mirrored in luminescence spectra presented in Fig. 7. At room temperature (Fig. 7a and b) excitation with 227 or 175 nm radiation produces very similar Tb^{3+} emission spectra with components located round about 382, 417, 440 and 460 nm attributed to the $^5D_3 \rightarrow {}^7F_{6/5/4/3}$ luminescence and constituents positioned at around 490, 544, 589 and 623 nm ascribed to the $^5D_4 \rightarrow {}^7F_{6/5/4/3}$ transitions. The situation changes at 10 K when both excitations generate emissions with different characteristics, though with some similarities. What all the emissions at 10 K have in common is the Tb^{3+} luminescence, with the characteristic structures related to radiative relaxation from the $^5D_3$ and $^5D_4$ states. In the case of the crystalline powder

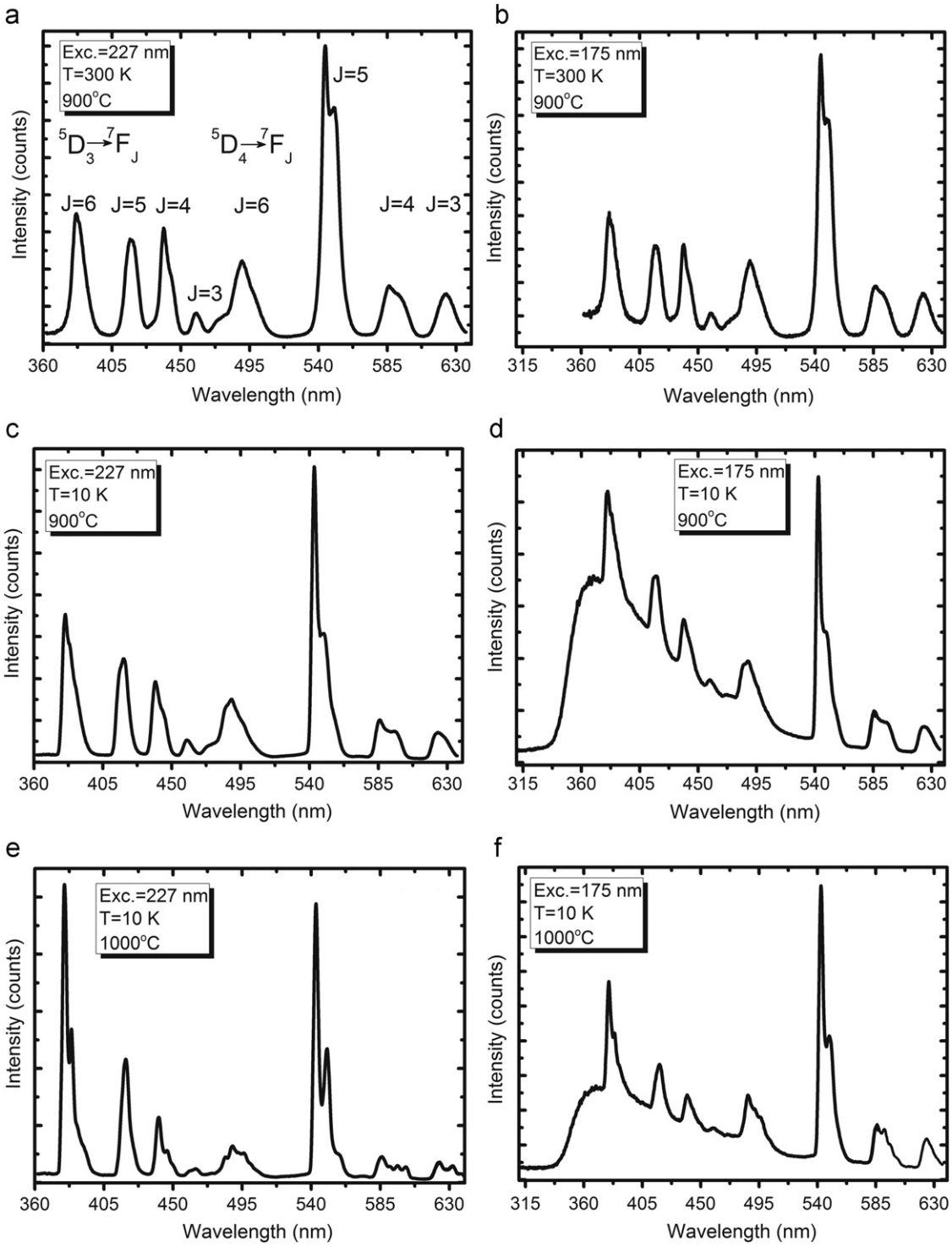

Fig. 7. Emission spectra of $Ca_3Y_2(Si_3O_9)_2$:Tb (1%) made at 900 °C recorded at room temperature (a, b) and 10 K (c, d) under excitation with 227 nm (a, c) and 175 nm (b, d) wavelength radiation. Emission spectra of $Ca_3Y_2(Si_3O_9)_2$:Tb (1%) prepared at 1000 °C recorded at 10 K under excitation with 227 nm (e) and 175 nm (f) wavelength radiation.

made at 1000 °C the emission features are much narrower indicating a diminished inhomogeneous broadening, as expected. A similar effect was seen in the excitation spectra (Fig. 6). Under stimulation with the high energy radiation of 175 nm a broad luminescence band of a significant intensity spreading from 350 to 500 nm appears (Fig. 7d and f). Such a spectral location makes the $4f \rightarrow 4f$ emissions of Tb^{3+} superimposed on this luminescent structure. The Stoke's shift of the excitation (175 nm) and emission (365 nm) is too large ($\sim$29 750 cm^{-1}) for electron–hole recombination. Hence, the concept presented in the discussion of results shown in Fig. 7 that this emission is connected with an exciton relaxing radiatively with the use of a defect appears indeed reasonable.

Stimulation with 227 nm wavelength radiation at 10 K leads to Tb^{3+} luminescence exclusively and the intensity of the more energetic emission from the $^5D_3$ level contains over 50% of the total, when the material is prepared at 1000 °C (Fig. 7e). For the powder made at 900 °C the $^5D_3$ luminescence comprises about 30% of the

entire intensity (Fig. 7c). The same was seen at RT indicating that the efficiency of the cross-relaxation responsible for feeding the $^5D_4$ state hardly changes between 10 K and RT. This may further imply that phonons do not play a significant role in the cross-relaxation process and consequently that this is the distance and capability of a direct interaction between the dopant ions, which appears to be the most important factor in the process.

4. Conclusions

Calcium yttrium silicate powders activated with Tb^{3+} were prepared with sol–gel method. Structural analysis revealed that pure monoclinic phase of $Ca_3Y_2(Si_3O_9)_2$ appears after heat-treatment at 1000 °C. The luminescent properties of singly doped $Ca_3Y_2(Si_3O_9)_2$:Tb upon stimulation in UV or VUV (synchrotron radiation) at room temperature and at 10 K were investigated. It was shown that the somewhat specific structure of the host material allowed receiving intense $^5D_3 \rightarrow {}^7F_J$ luminescence in blue violet and near-UV region even for relatively high Tb concentrations. Results of VUV spectroscopy show that at low temperature an excitonic state is formed and it can radiatively relax with the use of a defect giving broad band emission at around 365 nm. Measurements with synchrotron radiation revealed that luminescence of Tb^{3+}-doped $Ca_3Y_2(Si_3O_9)_2$ phosphors can be efficiently excited by stimulation of the host lattice. It was shown that the luminescence color could be tuned from yellowish-green to bluish-white by means of technological parameters.

Acknowledgments

The research was supported by the EU Program of Innovative Economy POIG.01.01.02-02-006/09. Partial support through DESY-HasyLab Grant #II-20090289 and EC and Minister of Science and Higher Education Grant #N N209 044839 is also acknowledged.

References

[1] H. Yamane, T. Nagasawa, M. Shimada, T. Endo, Acta Crystallographica C 53 (1997) 1533–1536.
[2] ICSD database, Version 1.4.6 2009-2.
[3] V.B. Mikhailik, Materials Letters 63 (2009) 803–805.
[4] G. Blasse, B.C. Grabmeier, Luminescent Materials, Springer-Verlag, 1994.
[5] K. Tonooka, K. Shimokawa, O. Nishimura, Solid States Ionic 151 (2002) 105–110.
[6] Yi-Chen Chiu, Wei-Ren Liu, Yao-Tsung Yeh, Shyue-Ming Jang, Teng-Ming Chen, Journal of Electrochemical Society 156 (2009) J221–J225.
[7] Yi-Chen Chiu, Wei-Ren Liu, Yao-Tsung Yeh, Shyue-Ming Jang, Teng-Ming Chen, ECS Transactions 25 (2009) 157–165.
[8] Z. Andric, R. Krsmanovic, M. Marinovic-Cincovic, T. Dramicanin, B. Secerov, M.D. Dramicanin, Acta Physica Polonica A 112 (2007) 969–974.
[9] A. Möller, P. Amann, Zeitschrift fur Anorganische und Allgemeine Chemie 627 (2001) 172.
[10] Boyer Vetrone, Capobianco, in: H.S. Nalwa, L.S. Rohwer (Eds.), Handbook of Luminescence, Display Materials and Devices, vol. 2, American Scientific Publishers, , 2003 ISBN:158883-031-4.
[11] P.J. Dereń, M.A. Weglarowicz, P. Mazur, W. Stręk, Journal of Luminescence 122–123 (2007) 780–783.
[12] K. Riwotzki, H. Meyssamy, A. Kornowski, M. Haase, The Journal of Physical Chemistry B 104 (2000) 2824–2828.
[13] E. Cavalli, P. Boutinaud, R. Mahiou, M. Bettinelli, P. Dorenbos, Inorganic Chemistry 49 (2010) 4916–4921.
[14] D. de Graaf, S.J. Stelwagen, H.T. Hintzen, G. de With, Journal of Non-Crystalline Solids 325 (2003) 29–33.
[15] P. Dorenbos, Journal of Luminescence 91 (2000) 91–106.
[16] L. van Pieterson, M.F. Reid, R.T. Wegh, S. Soverzo, A. Meijerink, Physical Review B 65 (2002) 045113.
[17] L. van Pieterson, M.F. Reid, G.W. Burdick, A. Meijerink, Physical Review B 65 (2002) 045114.
[18] G.H. Dieke, Spectra and Energy Levels of Rare Earth Ions in Crystals, Wiley Interscience, New York, 1968.
[19] M.N. Berberan-Santos, E.N. Bodunov, B. Valeur, Chemical Physics 315 (2005) 171–182.
[20] P. Boutinaud, P. Putaj, R. Mahiou, E. Cavalli, A. Speghini, M. Bettinelli, Spectroscopy Letters 40 (2007) 209–220.
[21] D. Wang, Y. Wang, Materials Chemistry and Physics 115 (2009) 699–702.